



This file is an uncorrected accepted manuscript (i.e., postprint). Please be aware that during the production process this version will definitively change. This postprint will be removed once the paper is officially published.

All legal disclaimers that apply to the journal pertain.

Submitted: 3 March 2023 - **Accepted:** 10 July 2023 - **Posted online:** 19 July 2023

To link and cite this article:

doi: 10.5710/AMGH.10.07.2023.3552

PLEASE SCROLL DOWN FOR ARTICLE

1 **TAPHONOMIC SIGNATURE OF *GLYCYMERIS LONGIOR* SHELLS**
2 **(BIVALVIA) AND ITS POTENCIAL AS PALEOENVIRONMENTAL PROXY**
3 **FOR QUATERNARY NORTHERN PATAGONIA (ARGENTINA)**

4

5 SOL BAYER^{1,2}, JULIETA C. NÓBILE^{1,2}, DIEGO F. MUÑOZ^{1,2}, ENRIQUE M.

6 MORSAN³, GISELA A. MORÁN^{1,4}, ENRIQUE FUCKS⁵, AND SANDRA

7 GORDILLO^{6,7}

8 ¹Facultad de Ciencias Exactas, Físicas y Naturales. Universidad Nacional de Córdoba.

9 Av. Vélez Sársfield 1611, X5016CGA, Ciudad Universitaria, Córdoba, Argentina.

10 ²Consejo Nacional de Investigaciones Científicas y Tecnológicas (CONICET), Centro

11 de Investigaciones en Ciencias de la Tierra, (CICTERRA). Av. Vélez Sársfield 1611,

12 Edificio CICTERRA, 1° Piso of. 18, X5016CGA, Ciudad Universitaria, Córdoba,

13 Argentina. sol.bayer@conicet.gov.ar; jnobile@unc.edu.ar; dmunoz@unc.edu.ar

14 ³Centro de Investigación Aplicada y Transferencia Tecnológica en Recursos Marinos

15 "Almirante Storni" (CIMAS), Universidad del Comahue-CONICET, Güemes 1030,

16 R8520CXV, San Antonio Oeste, Río Negro, Argentina. qmorsan@gmail.com

17 ⁴Consejo Nacional de Investigaciones Científicas y Tecnológicas (CONICET), Instituto

18 de Diversidad y Ecología Animal (IDEA). Av. Vélez Sarsfield 299, X5016GCA.

19 Córdoba, Argentina. gisela.amoran@gmail.com

20 ⁵Universidad Nacional de La Plata. Facultad de Ciencias Naturales y Museo y Ciencias

21 Agrarias y Forestales-LATYR-UNLP. Calle 64 N° 3, La Plata, (1900), Argentina.

22 efucks@fcnym.unlp.edu.ar

23 ⁶Universidad Nacional de Córdoba. Facultad de Filosofía y Humanidades. Museo de
24 Antropologías de Córdoba. Córdoba, Argentina.

25 ⁷Consejo Nacional de Investigaciones Científicas y Tecnológicas (CONICET), Instituto
26 de Antropología de Córdoba (IDACOR). Av. Hipólito Yrigoyen 174, X5000JHO,
27 Córdoba, Argentina. sandra.gordillo@unc.edu.ar

28

29 32 pag. (text + references); 6 figs.; 1 table

30

31 Running Header: BAYER *ET AL.*: *GLYCYMERIS LONGIOR* SHELLS AS

32 PALAEOENVIRONMENTAL PROXY

33 Short Description: Preservation patterns of *G. longior* assemblages corresponded to
34 various water flow energies, resulting in distinct carbonate precipitation.

35

36 Corresponding author: Sol Bayer, sol.bayer@conicet.gov.ar

37 **Abstract.** One of the most abundant species of bivalves found on modern beaches and
38 Quaternary deposits in the San Matías Gulf (SMG, Patagonia Argentina, SW Atlantic
39 Ocean) is *Glycymeris longior*. Its high abundance and broad geographical distribution
40 turn *G. longior* into a target species for taphonomical studies. Here, we described the
41 taphonomic signature registered on its shells from San Antonio Bay (SMG, Rio Negro).
42 This study will contribute to future taphonomic comparisons in the SW Atlantic Ocean,
43 as well as in other Quaternary deposits and provide insight about the spatial variation of
44 the taphonomic processes influenced by the ambient environment. *Glycymeris longior*
45 valves from the Holocene Punta Delgado deposits showed two taphonomic signatures
46 whose shell assemblages were differentiated by fragmentation, rounding and
47 cementation intensities. Shells from PD2018A and PD2018B (two sampling localities
48 representing similar environment) were subject to continuous and low energy water
49 flow. Those remained in a low intensity hydrodynamic sediment-water interface that
50 would favour high shell cementation. On the other hand, shells from PD2016 were also
51 subject to continuous, but more energetic water flow. Those would remain in the
52 taphonomic active zone for enough time to confer smooth edges and to be colonized by
53 clionid sponges but not enough favourable for carbonate precipitation. Punta Delgado
54 site was interpreted as a protected area during the Holocene (last 4200 yrs.) similar to
55 the modern one, but with differences in carbonate precipitation as the product of
56 differences in water flow intensities. Finally, the high mechanical resistance of *G.*
57 *longior* shells, together with its abundance and broad geographical distribution turn this
58 species into a suitable target taxon for further taphonomic and ecologic analyses and
59 comparisons.

60 **Keywords.** *Glycymeris longior*. Taphonomy. Cementation. Spit bars. Bay. Macrotidal
61 regime. Patagonia. Quaternary.

62 **Resumen. PERFIL TAFONÓMICO DE VALVAS DE *GLYCYMERIS LONGIOR***
63 **(BIVALVIA) COMO PROXI PALEOAMBIENTAL PARA EL CUATERNARIO**
64 **DE PATAGONIA NORTE (ARGENTINA).** Una de la especies de bivalvos más
65 abundantes que habita en la playas y depósitos cuaternarios del Golfo San Matías
66 (GSM, Patagonia argentina, Océano Atlántico sud occidental) es *Glycymeris longior*. Su
67 gran abundancia y amplia distribución geográfica, hace que *G. longior* sea una especie
68 objetivo para estudios tafonómicos. Por lo cual, describimos el perfil tafonómico que
69 registran sus valvas en la Bahía San Antonio (GSM, Argentina) con el objetivo de
70 contribuir a futuras comparaciones tafonómicas, con material de playas actuales o de
71 depósitos cuaternarios donde esta especie se encuentre. Las valvas de *G. longior* de los
72 depósitos holocenos de Punta Delgado mostraron dos patrones de preservación
73 diferentes caracterizados por diferencias en la intensidad de fragmentación,
74 redondeamiento y cementación de sus valvas. Las valvas de PD2018A y PD2018B
75 estuvieron sometidas a un flujo de agua continuo y poco intenso. Éstas permanecieron
76 en la interfase sedimento-agua con menor intensidad hidrodinámica lo que favorecería a
77 una alta cementación. Por otro lado, las valvas de PD2016 estuvieron sujetas también a
78 un flujo de agua continuo, pero más intenso o energético. Éstas permanecerían en la
79 TAZ el tiempo suficiente para producir bordes redondeados y ser colonizadas por las
80 esponjas cliónidas pero no lo suficientemente para la precipitación de carbonatos. El
81 sitio Punta Delgado se interpretó como una zona protegida durante el Holoceno (últimos
82 4200 años) similar a la actual, pero con diferencias en la precipitación de carbonatos

83 como producto de las distintas intensidades del flujo de agua. Finalmente, la alta
84 resistencia mecánica de las valvas de *G. longior*, junto con su abundancia y amplia
85 distribución geográfica convierten a esta especie en un taxón adecuado para análisis y
86 comparaciones futuras.

87 **Palabras clave.** *Glycymeris longior*. Tafonomía. Cementación. Espigas litorales. Bahía.
88 Régimen macromareal. Patagonia. Cuaternario.

89 THE SAN MATÍAS GULF (SMG), located on the northeastern coast of Patagonia (Fig.
90 1.1), Argentina, has a rich mollusc fossil record throughout the Quaternary. To the north
91 of the SMG, at 40°45'S, the semicircular San Antonio Bay encompasses modern and
92 old coastal environments with muddy tidal flats and spits of gravel and sand (Carbone *et*
93 *al.* 2007). The morphology of the bay is a result of a submerged depression and the
94 development of coastal features such as spit bars and beach ridges throughout the
95 Quaternary transgressions and regressions (Angulo *et al.* 1978; Rutter *et al.* 1989, 1990;
96 Favier-Dubois & Kokot 2011; Fucks *et al.* 2012; Mouzo 2014). A detailed study of the
97 comparative taphonomy of molluscan shell assemblages may provide insight about the
98 Quaternary coastal dynamics in which these deposits developed.

99 Modern and Quaternary molluscan assemblages from beaches associated to soft
100 bottoms from San Antonio Bay are characterized by the predominance of two bivalve
101 species: *Eucallista purpurata* (commonly known as *Amiantis purpurata*) that dominates
102 the eastern side of the bay, and *Glycymeris longior* on the western side. In previous
103 studies, taphonomic and paleoecologic analyses of *E. purpurata* allowed the
104 reconstruction of the paleoenvironmental conditions during the Quaternary (Bayer *et al.*
105 2013, 2015, 2016) in those assemblages where this species was dominant. Physical,
106 biological and even anthropogenic factors would have changed through time coinciding
107 with local and global events such as: the Last Glacial Maximum, the final configuration
108 of the coast of the SMG, and the Holocene Climatic Optimum (Bayer *et al.* 2016, 2020).
109 At the same time, *G. longior* is an abundant species in the Quaternary marine coastal
110 assemblages and modern beaches. Empty *G. longior* valves are found in high
111 proportions on the beach; their shells are some of the most robust and resistant in the

112 mollusc assemblages (López *et al.* 2008; Boretto *et al.* 2013; Bayer *et al.* 2016). This
113 species presents a broad continuous geographical distribution from Pará State (Brazil) in
114 the north to the northern SMG in Argentina (Farinati 1978; Rocha & Matthews-Cascon
115 2014; WoRMS Editorial Board 2023), and it is found in great abundance in the study
116 area. The advantage of considering a target species for taphonomic analysis, i.e. the
117 same species from different assemblages throughout the same region, is the elimination
118 of interspecific variations associated with intrinsic factors such as the shell's
119 microstructure, life habits and behavior, among others (Bayer *et al.* 2016, 2019). Thus,
120 the purpose of this study is to describe the taphonomical signature registered on *G.*
121 *longior* shells from San Antonio Bay (SMG, Rio Negro), as a target species to
122 contribute to future taphonomical comparisons in SW Atlantic Ocean, as well as in
123 other Quaternary deposits in which it can be found. Also, we evaluated the geology and
124 geomorphology of the San Antonio Bay area, together with taphonomic interpretations,
125 to understand the depositional environment and timing of the deposits.

126

127 **MATERIAL AND METHODS**

128 **Study area**

129 The SMG is the largest gulf in Patagonia, and one of the largest in South America
130 (Moreira *et al.* 2009). This gulf constitutes a semi-enclosed depression, whose bottom,
131 with depths close to 200 m, exceeds those corresponding to the edge of the shelf for that
132 same latitude (Pierce *et al.* 1969; Gagliardini *et al.* 2005; Ruiz Etcheverry *et al.* 2016;
133 Gordillo *et al.* 2018). Its water circulation behaves as a clockwise coastal eddy
134 predominantly influenced by tidal currents (Lanfredi & Pousa 1988; Tonini & Palma

135 2011), resulting in a protected area. . The San Antonio Bay is located in the north-
136 western area of the SMG (40°42'/40°50' S and 64°43'/65°07' W) (Fig. 1.1), partially
137 closed off by two spit bars (Fucks *et al.* 2012; Kokot & Favier-Dubois 2017). It
138 corresponds to a tidal marsh (Carbone *et al.* 2007) which can be described as shallow
139 inland marine waters, predominantly oriented parallel to the coast, separated from the
140 ocean by a barrier, and connected to the open sea by one or more restricted inlets. At the
141 inlet of San Antonio Bay, a tidal delta develops to depths of 14 m (Aliotta *et al.* 2000).
142 This bay is characterized by semidiurnal tides. It has a macrotidal regime which can
143 reach 9.22 m maximum in spring tide (SHN 2018).

144 The study site, Punta Delgado (40°45'10.89" S; 64°54'57.58" W), is located in the
145 western spit bar of the internal area of San Antonio Bay (Fig. 1.2). Punta Delgado is a
146 Pleistocene marine spit bar with Pleistocene and Holocene beach ridges composed
147 mainly of mollusc shells, along with gravel and sand overlain by modern dunes (Angulo
148 *et al.* 1978; Fucks *et al.* 2012; Kokot & Favier-Dubois 2017).

149 **Geological background of the SMG**

150 The SMG is located between the southwestern end of the Colorado Basin and the
151 Somuncurá Plateau elevations (Fig. 2). This depression can be considered part of the
152 Salinas Trapalcó-Laguna Curicó Lineament with an NW-SE trend (Fig. 2.1) (Turner &
153 Baldis 1978; Gregori *et al.* 2008). The San Antonio bay itself would be one of these
154 depressions (embayments) repeatedly flooded during the Quaternary (Porro & Fidalgo
155 1982; González Díaz & Malagnino 1984; Kokot & Favier Dubois 2009). The successive
156 Quaternary transgressive and regressive episodes imprinted different geomorphological
157 features (Angulo *et al.* 1978; Martínez *et al.* 2001; Fucks *et al.* 2012) such as beach

158 ridges, spits, littoral barriers, broad tidal flats, marshes and sandbanks (Fig. 2.3). The
159 San Antonio Bay is a tidal delta separated from the sea by two spit bars (Punta Delgado
160 to the West and Península Villarino to the East). They are elongated sand, gravel and
161 shell barriers that extend laterally through the construction of progradational beach
162 ridges (Davis & FitzGerald 2004). Along this internal channel, accumulative areas are
163 recognize forming curvilinear shore beach ridges (Fig. 1.2 and 1.3). This curvilinear
164 pattern is the consequence of refracted waves propagating through an inlet channel and
165 into the back-barrier region (Hine 1979; Costas & FitzGerald 2011; Isla *et al.* 2023). In
166 particular, sampling localities are located on the northern margin of the Punta Delgado
167 spit bar (Fig. 1.2).

168 Feruglio (1933, 1950) was the first to described the complete morphology, lithology,
169 palaeontology and relative chronology of the Quaternary marine terraces throughout
170 most of the Argentinean Patagonia coast. Then, Angulo *et al.* (1978) divided the
171 quaternary stratigraphy into two lithostratigraphic units: Baliza de San Matías and San
172 Antonio formations (Fig. 2.2) and assigned them to Pleistocene and Holocene
173 respectively. Regarding age control, these units were dated using radiocarbon dating
174 techniques (Angulo *et al.* 1981) with ages ranging between 27 ka and 40 ka, but this can
175 only provide a minimum age constraint to the Pleistocene. Rutter *et al.* (1989, 1990)
176 provided Aminostratigraphy and Electron Spin Resonance (ESR) dating from some
177 locations and concluded that deposits located at 24 m a.m.s.l. yielded ages between 169
178 ka and 230 ka (MIS 7), 83.2 ka-111 ka for deposits at 10 m a.m.s.l (MIS 5), and 66.8-
179 70.3 ka for beach rock (abrasion) platform at 0 m a.m.s.l. Both Baliza de San Matías
180 Fm. (MIS7) and San Antonio Fm. (MIS5e) are therefore assigned to the Pleistocene.

181 Based on these studies, Fucks et al. (2012) summarized the presence of four
182 transgressive events. The oldest transgressive event corresponds to Marine Isotope
183 Stage 9 (\geq MIS 9?) and its deposits are found 60-70 m a.m.s.l. and 10 km northwest of
184 San Antonio Oeste on the Provincial Road 2. The transgressive episode during the
185 middle Pleistocene (MIS 7, between 230 and 190 ka) was identified at three locations:
186 Caleta Falsa, Baliza Camino and northwest of San Antonio Oeste (Angulo *et al.* 1978;
187 Rutter *et al.* 1989, 1990). In San Antonio Bay MIS 5e (about 130-115 ka) shoreline
188 deposits and landforms are located between 12-8 m a.m.s.l. (Rutter *et al.* 1989, 1990;
189 Gowan *et al.* 2021) and covered the spit bars and the beach ridges (Baliza San Matías,
190 Puerto de Vialidad, La Rinconada, and on Provincial Road 2 near Gas Station). The
191 coast was an open sea environment subject to a tidal regime. During the Last Glacial
192 Maximum (LGM, 25–20 ka) (Hulton *et al.* 2002) the bay completely emerged, and
193 beach ridges were successively formed as the sea level dropped. From the early
194 Holocene (~11 ka) to the present the San Antonio Bay has been more protected from the
195 open sea (Ponce *et al.* 2011; Fucks *et al.* 2012). In San Antonio Bay beach ridges below
196 10 m a.m.s.l. are designated as Holocene, and beach ridges at higher altitudes as
197 Pleistocene. In particular, coarse sediments beach ridges in San Antonio Bay were
198 formed during high-energy storm waves inundating the coast (Carter, 1988; Taylor &
199 Stone, 1996; Tamura, 2012). They are formed mainly by shells with scarce sand matrix.
200 Beachface in Punta Delgado and Punta Perdices tends to be steeper (~23°) due to
201 coarser grain sizes (Bristow and Pucillo, 2006).

202 **Autoecology of *Glycymeris longior***

203 *Glycymeris longior* is a warm-temperate species whose modern distribution extends
204 from Pará State (Brazil) to the northern SMG in Argentina (Farinati 1978; Rocha &
205 Matthews-Cascon 2014; WoRMS Editorial Board 2023). It is an infaunal suspension
206 feeder living in fine and medium sandy bottoms, partially covered by small shell
207 particles (Ituarte 1979; Scarabino *et al.* 2006; Gimenez *et al.* 2020a, b). The
208 southernmost living population is found at El Sótano, in the NW sector of the SMG
209 (Fig. 2.3), at water depths from 6 to 20 m (Scarabino 1977), where sea water
210 temperature ranges from 8.3°C (in August) to 22.2°C (in January), and salinity ranges
211 from 34 to 36 ‰ (Pascual *et al.* 2001). The *G. longior* fossil record extends back to the
212 late Pleistocene in San Antonio Bay but has also been found in Quaternary deposits
213 from Buenos Aires province, Uruguay and Brazil (Farinati 1978; Lorenzo & Verde
214 2004; Clavijo *et al.* 2005; de Souza *et al.* 2010; Lopes *et al.* 2013; Bayer *et al.* 2016;
215 Martínez *et al.* 2016).

216 **Study materials**

217 The material was collected from two Holocene beach ridges at Punta Delgado (Fig. 1.2),
218 where *G. longior* is the most abundant species in the shell assemblages (Fig. 3).
219 Samples were collected superficially by hand at the top of the beach ridges. In order to
220 compare the taphonomic profile of different shell assemblages, samples were collected
221 by hand from 0.25 m² surface quadrat at two different beach ridges: PD 2016 and PD
222 2018A. Then, in order to compare sampling methods, we collected a third sample in the
223 same beach ridge as PD2018A. The third sample, PD2018B, represented 10 meters of a
224 continuous line transect (50 cm wide) of collecting superficially also by hand. These

225 samples contained materials bigger than 2 mm size. Deposits did not show evidence of
226 cementation nor consolidation.

227 **Taphonomic attributes studied in *Glycymeris longior***

228 For the choice of taphonomic attributes and taphonomic grades corresponding to this
229 species, various sources were consulted (Brett & Baird 1986; Kidwell *et al.* 1986;
230 Kidwell & Bosence 1991; Gordillo *et al.* 1993; Kowalewski *et al.* 1995; Zuschin *et al.*
231 2003; Gordillo 2009; Ritter *et al.* 2013, 2016; Bayer *et al.* 2016, 2019, among others).
232 The taphonomic attributes of the specimens were described using taphonomic grades
233 when quantifiable, or binary character states. In binary character states, zero
234 corresponds to a low-impacted or pristine state while one corresponds to an altered state
235 (Fig. 4; Supplementary material).

236 Fragmentation. This attribute is associated with shell breakage due to the action of
237 mechanical stress. It can be influenced by waves (Hollmann 1966; Parsons & Brett
238 1991; Smith & Nelson 2003) and biological interactions such as predation and
239 bioturbation (Zuschin *et al.* 2003). This attribute was coded as not fragmented (0), shell
240 breakage lower than 30% of the intact shell surface area (1), or shell breakage higher
241 than 30% (2).

242 Corrosion. This attribute was coded as original ornamentation (0) or corroded (1) when
243 superficial ornamentation was lost, or surface shell layers were exposed.

244 Rounding. This attribute is associated with exposure time. Shells may not lie far from
245 their point of origin but may have rolled back and forth over long distances (Smith &
246 Nelson 2003). Such oscillation of shells produces worn shell edges. Rounding was
247 classified as no rounding (0), and shells with rounded edges (1).

248 Domichnia traces. Some bioerosion structures were recognized on *G. longior* valves,
249 that can be assigned to the dwelling traces (Domichnia) ethological category.
250 Bioerosion structures found on infaunal bivalves, such as *G. longior*, are normally
251 produced *post-mortem* and after suffering transport, particularly after disarticulation
252 (Santos & Mayoral 2008). *Post-mortem* traces was coded as no presence (0), and
253 presence (1).
254 Other taphonomic attributes were coded as presence (1) or absence (0), namely external
255 surface cementation and internal surface cementation. Right and left valves were not
256 discriminated because they do not have significant assymetry in shell sculpture
257 (Chattopadhyay et al. 2013).
258 To explore differences in taphonomic signals among samples from different beach
259 ridges and sampling method, we used a non-metric multidimensional scaling analysis
260 (NMDS) calculated on Bray-Curtis dissimilarity index (square-rooted to made metric).
261 This analysis was implemented with the metaMDS function in the ‘vegan’ package
262 (version 2.6-4) for R software. We used a Multivariate Analysis of Variance with
263 Permutation (PERMANOVA) (Anderson 2001; Warton et al. 2012) with 9999
264 permutations to test for significant differences in preservation of bivalve assemblages
265 between the three samples. We carried out PERMANOVA with Bonferroni correction
266 for multiple comparissons, to test whether the three samples differ in preservation
267 pattern. All statistical tests were conducted in the R program (R Development Core
268 Team 2023, version 4.3.0).

269 **RESULTS**

270 We collected 517 valves of *G. longior* for the taphonomical study. Sample PD2016
271 contained 354 valves, PD2018A contained 73 valves and PD2018B had 90 valves.
272 The NMDS ordination clearly segregated PD2016 from PD2018A and PD2018B (Fig.
273 5), with PD2018A and PD2018B exhibiting more tightly clustered in the NMDS bi-
274 dimensional space/representation, with respect to sample PD2016.
275 PERMANOVA test also demonstrated significant differences between sample PD2016
276 with respect to PD2018A and PD2018B ($p < 0.0001$; $F = 42.22$). However, samples
277 PD2018A and PD2018B, collected with different methodologies (see Mat & Met
278 section), showed no significant differences between them (Table 1). Therefore, both
279 sampling methods did not show significant differences, then, did not contribute to the
280 definition of preservation patterns.
281 Two preservation patterns could be observed in samples' preservation profiles (Fig. 6).
282 In one hand, PD2016 was characterized by high fragmentation (67%) and low rates of
283 internal and external cementation (6 % and 14 % respectively). Also, it showed low
284 rounding rate (64%).
285 On the other hand, PD2018A and PD2018B were characterized by lower fragmentation
286 (34% and 32% respectively) than PD2016. Also, PD2018A and PD2018B showed
287 higher rates of rounding (93% and 96% respectively), presence of internal cementation
288 (91% and 94% respectively) and external cementation (86% and 95% respectively) than
289 PD2016.
290 However, shells from all three samples showed high rates of corrosion (PD2016: 89%;
291 PD2018A: 84%; PD2018B: 100%) and high presence of *Domichnia* traces (PD2016:
292 65%; PD2018A: 70%; PD2018B: 76%) (Fig. 6).

293 Therefore, there were two taphonomic patterns: PD2016 with high fragmentation and
294 low cementation; while PD2018A and PD2018B with low fragmentation but high
295 rounding and high degree of cementation.

296

297 **DISCUSSION**

298 The samples of *G. longior* shells from Punta Delgado showed two types of preservation
299 patterns which allow for the reconstruction of the paleoenvironment in the Holocene of
300 the SMG. The environmental factors affecting the different assemblages have left a
301 signature on the shell preservation at a different intensity (according to Brett & Baird
302 1986; Kidwell & Bosence 1991; Bayer et al. 2019).

303 The Punta Delgado (SMG) samples showed high percentages of bioerosion represented
304 by dwelling traces. These trace fossils, present in more than 65% of *G. longior* shells,
305 were probably produced by clionaid sponges (Bromley 2004; Belaústegui *et al.* 2012;
306 Gastaldi *et al.* 2018). *G.* is an infaunal bivalve which excavates shallow in the sediment
307 (Scarabino 1977), and lives buried on the first centimeters of it (Gimenez *et al.* 2020).

308 On the other hand, sponges are epifaunal organisms; therefore these dwelling traces
309 would have been made when *G. longior* shells were exhumed and exposed on the
310 seafloor. Thus, colonization by sponges must took place after the death of the *G. longior*
311 shells. After death, the valves were exhumed, disarticulated and separated facilitating
312 the settlement of these bioeroders on shell surfaces (Santos & Mayoral 2008;
313 Belaústegui *et al.* 2018). Exhumed infaunal bivalve shells would be expected to have
314 encrustation on interior surfaces only after their death and exhumation (Lescinsky *et al.*
315 2002). Moreover, most of the *G. longior* shells showed a high intensity of *post-mortem*

316 traces, reflecting that these shells were exposed to the water-sediment interface for a
317 sufficient amount of time, allowing bioeroders to colonize the valves (Bromley *et al.*
318 1990; Lescinsky *et al.* 2002; Santos & Mayoral 2008). That slow initial colonization
319 would be carried out by these boring organisms during the first 1-2 years (Bromley &
320 De Alessandro 1990; Bromley *et al.* 1990; Peyrot-Clausade *et al.* 1995; Walker *et al.*
321 1998). Moreover, *G. longior* shells exhibited a high boring intensity, which may
322 indicate that these shells were exposed to the sediment-water interface for several years
323 after death at least once, either by storms, tides or wave action and/or bioturbation
324 (Parsons-Hubbard *et al.* 1999; Rodland *et al.* 2006). According to the taphonomic
325 profile of the assemblages, we suggest here that exhumation of shells could have
326 occurred several times.

327 *G. longior* shells exhibited high proportion of shells with smooth surfaces, which could
328 suggest the presence of other components in the water that also intervened in the
329 corrosion of the shells. We propose that water currents containing suspension particles,
330 such as sand grains, grounded and eroded shell surfaces and edges. Moreover, shells
331 also exhibited a high proportion of rounded edges. Besides waves and tides that
332 produced shell abrasion, the factor of exposure time was implied here favoring worn
333 shell edges. *G. longior* shells may have been subjected to transport but also may have
334 rolled back and forth (Smith & Nelson 2003), oscillating on the water-sediment
335 interface. Despite the fact that the three samples exhibited high corrosion, rounding and
336 presence of *post-mortem* traces, they showed different taphonomic signatures. Sample
337 PD 2016 can be differentiated from PD 2018A and PD 2018B, primarily based on
338 fragmentation, rounding and internal and external cementation.

339 Shells from PD2016 showed higher fragmentation than shells from PD2018A and
340 PD2018B. Taking into account that this taphonomic attribute is related to mechanical
341 stress (Hollmann 1966; Brett & Baird 1986; Parsons & Brett 1991), water flow could be
342 a significant environmental factor. In terms of fragmentation, these currents could have
343 been accompanied by big particles such as shell fragments, which struck and broke *G.*
344 *longior* valves (Brett & Baird 1986; Parsons & Brett 1991). Therefore, during the
345 biostratinomic phase, the environment of Punta Delgado had been subjected to tides and
346 wave action contributing to the high fragmentation of shells which would have been
347 transported by more energetic episodes such as storms and led to the accumulation on
348 the beach ridge where PD2016 belong.

349 On the other hand, shells from PD2018A and PD2018B exhibited a similar
350 taphonomical profile between them characterized by low fragmentation, high rounding
351 and internal and external cementation. Their rounding edges and high abrasion suggest
352 that shells were oscillating on the water-sediment interface and were accumulated *post-*
353 *mortem* in the wave/tidal zone as a loose material similar to those from PD2016.
354 However, low fragmentation and high rates of rounding suggest that water currents
355 contain suspended particles, such as sand grains, ground and eroded shell surfaces and
356 edges but in a minor intensity or energy than PD2016 assemblage suffered. The high
357 rates of internal and external cementation on PD2018A and PD2018B shells indicate
358 that the water flow allowed the mobility of shells within the wave zone and/or tidal
359 zone, where their cementation would occur (Moresby 1835; Hanor 1978; Hopley 1986;
360 Vousdoukas *et al.* 2007). As other studies have shared, cementation could be achieved
361 under specific physical-chemical-microbial conditions in a tidal or immediately supra-

362 tidal environment depending on seawater temperatures, evaporation, mixing of seawater
363 with meteoric and groundwater, wetting and drying, microbiological activity and upon
364 the concentration of seawater CO_3^{2-} (Schmalz 1971; Molenaar & Venmans 1993;
365 Stoddart & Cann 1995; Turner 2005; Vousdoukas *et al.* 2007; Mauz *et al.* 2015).

366 Therefore, the bivalve death assemblages from the beach ridge where PD2018A and
367 PD2018B belong, detect a more favorable environment for carbonate precipitation than
368 the beach ridge where PD2016 belong.

369 Today, San Antonio Bay is subject to periodic storms with southeast winds and strong,
370 high waves that produce coastal erosion (Kokot *et al.* 2004). Furthermore, this bay
371 exhibits a hydraulic regimen determined by semi-diurnal tides, with a maximum spring
372 tide of 9.56 m (Aliotta *et al.* 2000; SHN 2018). Tide currents have maximum values
373 recorded at 2 m/sec (SHN 2018), which is a high-energy environment where intertidal
374 banks are subject to intense morphodynamic processes (Isla *et al.* 1995; Moreira *et al.*
375 2011). However, today the Punta Delgado site is not affected by storms or wave action,
376 and is actually a low-energy environment and a protected area due to its geomorphology
377 (Fucks *et al.* 2012; Kokot & Favier-Dubois 2017). Only extraordinary high tide can
378 reach the shore in Punta Delgado, leaving a backwash at 9.30 m, where the study site is
379 not affected by tidal flows (pers. observ.; Fig. 3.6). Also, this site is located in the
380 northern margin of the Punta Delgado spit bar, where the refraction of waves
381 propagating through the inlet channel generated these curvilinear beach ridges parallel
382 to the shoreline (see Fig. 1.2).

383 During the Holocene, beach ridges started to be accumulated on the Pleistocene spit bar
384 of Punta Delgado. However, there were some differences in the preservation pattern of
385 shells from adjacent beach ridges which would correspond to different history or
386 taphonomic setting. When considering that both sampled beach ridges are located in an
387 active coastal environment, inland beach ridges tend to be older than seaward beach
388 ridges. Thus, the beach ridge where PD2018A and PD2018B were taken, would be
389 older than the beach ridge where PD2016 was taken. The shells of PD2018A and
390 PD2018B were subject to continuous, less intense water flow charged with smaller
391 particles. Consequently, the valves resulted in longer time remaining in the
392 taphonomically active zone. Longer time in a less intense hydrodynamic sediment-water
393 interface, with other environmental factors, would favour higher shell cementation. On
394 the other hand, shells from PD2016 were subject also to continuous but more intense or
395 energetic water flow, such as wave action, and charged with bigger particles. Shells
396 would remain in the TAZ for enough time to confer smooth edges and to be colonized
397 by clionid sponges. However, environmental factors were not suitable for cementation
398 for PD2016.

399 We propose that Punta Delgado is a Pleistocene spit bar with Holocene large deposits
400 which exhibit extensive long-term time-averaging of mostly *G. longior* shells. This site
401 is the product of a complex history of transport and reworking of materials (Kidwell
402 2013), in a Holocene environment affected mostly by spring tides. A previous study in
403 San Antonio Bay, using a bivalve species as a target taxon, found that the taphonomic
404 signature of the *E. purpurata* shells was also interpreted as a low-energy environment
405 with varying intensity depending on the locality (Bayer *et al.* 2016). The transported

406 and reworked material of *E. purpurata* indicated an earlier deposition and, also, at least
407 one storm event (Bayer *et al.* 2016). Thus, considerable time-averaging was observed
408 in those associations from San Antonio Bay (especially in the eastern side, Punta
409 Villarino) (Fürsich and Aberhan, 1990; Kidwell, 1991; 2013). In our study, the western
410 side of San Antonio Bay, the taphonomical pattern of *G. longior* assemblages from both
411 beach ridges of Punta Delgado are characterized by the differences in shell rounding
412 and cementation corresponding to differences in the water flow intensity, coinciding
413 with Bayer *et al.* (2016) proposed studying *E. purpurata* as target species.

414 The intense water currents caused by sporadic storms and spring tides in Punta Delgado
415 could have produced mechanical reworking and selection of materials which have a
416 specific composition and mechanical resistance (Chave 1964; Cadée 1968; Bayer *et al.*
417 2016). The high concentrations of *G. longior* on the beach could be due to its very thick,
418 planar shape (López *et al.* 2008), as well as a cross lamellar microstructure that confers
419 higher mechanical strength (Rhoads & Lutz 1980; Bolmaro *et al.* 2006; Boretto *et al.*
420 2013). These characteristics allowed *G. longior* to persist over time and to withstand
421 transport and weather conditions in the swash zone (López *et al.* 2008). The high
422 mechanical resistance of *G. longior*, together with the high shell supply, could have
423 produced large deposits. However, other species whose shells have low mechanical
424 strength would not be found at all or would be found in low proportions. Therefore, *G.*
425 *longior*, a common warm-temperate species that is also abundant in marine Quaternary
426 deposits (Bayer *et al.* 2016) serves as a useful target taxa for future taphonomic
427 comparisons.

428 **CONCLUSIONS**

429 - *Glycymeris longior* valves from Holocene Punta Delgado deposits showed two
430 taphonomic signatures, in terms of fragmentation, rounding and cementation
431 differences.

432 - Shells from PD2018A and PD2018B were subject to continuous and low
433 energy water flow. Those remained in a less-intensity hydrodynamic sediment-
434 water interface that would favour high degree of cementation. Shells from
435 PD2016 were subject also to continuous but more intense or energetic water
436 flow. Those would remain in the taphonomically active zone for enough time to
437 confer smooth edges and to be colonized by clionid sponges but not enough
438 favourable for carbonate precipitation.

439 - The Punta Delgado site was interpreted as a protected area during the Holocene
440 (last 4200 yrs.) similar to the modern one, but with differences in carbonate
441 precipitation as the product of differences in water flow intensities.

442 - The high mechanical resistance of *G. longior* shells, together with the high
443 shell supply, produced large deposits in Punta Delgado spit bar.

444 **ACKNOWLEDGMENTS**

445 We would like to thank Dr María del Socorro Doldán (Universidad Nacional del
446 Comahue-CIMAS-CONICET) for her invaluable help in different field trips. We
447 acknowledge Ivana Tapia (CICTERRA) for help with shells' photographs. Authors also
448 acknowledge anonymous reviewers as well as the Associate Editor Devapriya
449 Chattopadhyay for their rich and interesting contributions.

450 **REFERENCES**

- 451 Aliotta, S., Schnack, E.J., Isla, F. and Lizasoain, G.O. 2000: Desarrollo secuencial de
452 las formas de fondo en un regimen macromareal. *Asociacion Argentina de*
453 *Sedimentologia* 7, 95–107.
- 454 Anderson, M.J. 2001: A new method for non-parametric multivariate analysis of
455 variance. *Austral Ecology* 16, 32–46.
- 456 Angulo, R., Fidalgo, F., Gomez Peral, M. and Schnack, E.J. 1981: Geología y
457 geomorfología del Bajo San Anotnio y alrededores, Provincia de Rio Negro. 33.
- 458 Angulo, R.J., Fidalgo, F., Gomez Peral, M. and Schnack, E.J. 1978: Las ingresiones
459 marinas cuaternarias en la Bahia San Antonio y sus vecindades, Provincia de Rio
460 Negro. *Acta del 7° Congreso Geológico Argentino* 1, 271–283.
- 461 Bayer, S., Beierlein, L., Morán, G.A., Doldán, M.S., Morsan, E.M., Brey, T.,
462 Mackensen, A., Farias, L., García, G. and Gordillo, S. 2020: Late Quaternary
463 climatic variability in northern Patagonia, Argentina, based on $\delta^{18}\text{O}$ of modern and
464 fossil shells of *Amiantis purpurata* (Bivalvia, Veneridae). *Palaeogeography,*
465 *Palaeoclimatology, Palaeoecology* 560, 110012.
- 466 Bayer, S., Balseiro, D., Muñoz, D.F. and Gordillo, S. 2019: Unveiling the consequences
467 of environmental variation and species abundances on beach taphofacies in
468 Bahamas: the role of cementation and exhumation. *Palaios* 34, 300–316.
- 469 Bayer, S., Gordillo, S. and Morsan, E. 2016: Late Quaternary faunal changes in
470 northeastern Patagonia (Argentina) according to a dynamic mosaic of benthic
471 habitats: taphonomic and paleoecological analyses of mollusk assemblages.
472 *Ameghiniana* 53, 655–674.
- 473 Bayer, S., Morsan, E., Gordillo, S. and Moran, G. 2015: Form changes in *Amiantis*
474 *purpurata* (Bivalvia, Veneridae) shells over the past 100,000 years in North
475 Patagonia (Argentina). *Journal of the Marine Biological Association of the United*
476 *Kingdom* 96, 1243–1250.
- 477 Bayer, S., Colombo, F., De Vincentis, N.S., Duarte, G.A., Bolmaro, R. and Gordillo, S.
478 2013: Cryptic diagenetic changes in Quaternary Aragonitic shells: a textural,
479 crystallographic, and trace-element study on *Amiantis purpurata* (Bivalvia) from
480 Patagonia, Argentina. *Palaios* 28, 438–451.
- 481 Belaústegui, Z., Domènech, R. and Martinell, J. 2018: An ichnofossil-lagertätte from
482 the Miocene Vilanova Basin (NE Spain): taphonomic and paleoecologic insights
483 related to bioerosion structures. *Palaios* 33, 16–28.

- 484 Belaústegui, Z., Nebelsick, J.H., De Gibert, J.M., Domènech, R. and Martinell, J. 2012:
 485 A taphonomic approach to the genetic interpretation of clypeasteroid
 486 accumulations from the Miocene of Tarragona, NE Spain. *Lethaia* 45, 548–565.
- 487 Boretto, G.M., Gordillo, S., Cioccale, M., Colombo, F. and Fucks, E.E. 2013: Multi-
 488 proxy evidence of Late Quaternary environmental changes in the coastal area of
 489 Puerto Lobos (northern Patagonia, Argentina). *Quaternary International* 305, 188–
 490 205.
- 491 Bolmaro, R.E., Romano Trigueros, P. and Zaefferer, S. 2006: Estudio de la resistencia
 492 mecánica y la textura de los caparazones mineralizados de bivalvos. 17º
 493 CBECiMat - Congresso Brasileiro de Engenharia e Ciência dos Materiais, 11646–
 494 11654.
- 495 Brett, C.E. and Baird, G.C. 1986: Comparative taphonomy; a key to paleoenvironmental
 496 interpretation based on fossil preservation. *Palaios* 1, 207–227.
- 497 Bristow, C.S. and Pucillo, K., 2006. Quantifying rates of coastal progradation from
 498 sediment volume using GPR and OSL: the Holocene fill of Guichen Bay, south-
 499 east South Australia. *Sedimentology* 53, 769–788.
- 500 Bromley, R.G. 2004: A stratigraphy of marine bioerosion. 1. In McIlroy, D. (ed.), *The*
 501 *Application of Ichnology to Palaeoenvironmental and Stratigraphic Analysis, Vol.*
 502 228, 455–479. The Geological Society of London, London.
- 503 Bromley, R.G. and De Alessandro, A. 1990: Comparative analysis of bioerosion in
 504 deep and shallow water, Pliocene to Recent, Mediterranean Sea. *Ichnos* 1, 43–49.
- 505 Bromley, R.G., Hanken, N.-M. and Asgaard, U. 1990: Shallow marine bioerosion:
 506 preliminary results of an experimental study. *Bulletin of the Geological Society of*
 507 *Denmark* 38, 85–99.
- 508 Cadée, G.C. 1968: Molluscan biocenoses and thanatocenoses in the Ria De Arosa,
 509 Galicia, Spain. *Zoologische Verhandelingen* 95, 1–21.
- 510 Carbone, M.E., Perillo, G.M.E. and Piccolo, M.C. 2007: Morphological dynamics of
 511 costal environments of San Antonio Oeste Bay, Rio Negro Province. *Geoacta* 32,
 512 83–91.
- 513 Carter, R.W.G., 1988. Coastal Environments. *Academic press, London*. 617 p.
- 514 Chattopadhyay, D., Rathie, A. and Das, A. 2013: The effect of morphology on
 515 postmortem transportation of bivalves and its taphonomic implications. *Palaios* 28,
 516 203–209.

- 517 Chave, K.E. 1964: Skeletal durability and preservation. *In* Imbrie, J., Newell, N. (eds.),
518 *Approaches to Paleoecology*, 377–387. John Wiley and Sons Inc, New York.
- 519 Clavijo, C., Scarabino, F., Rojas, A. and Martínez, S. 2005: Lista sistemática de los
520 moluscos marinos y estuarinos del Cuaternario de Uruguay. *Comunicaciones de la*
521 *Sociedad Malacológica del Uruguay* 9, 381–411.
- 522 Costas, S. and FitzGerald, D.M. 2011: Sedimentary architecture of a spit-end (Salisbury
523 Beach, Massachusetts): The imprints of sea-level rise and inlet dynamics. *Marine*
524 *Geology* 284, 203–216.
- 525 Davis, R.A. and FitzGerald, D.M. 2004: *Beaches and Coasts*. Blackwell,
526 Massachusetts, 419p.
- 527 Farinati, E. 1978: Microfauna de moluscos Querandinenses (Holoceno) de Ingeniero
528 White, provincia de Buenos Aires. *Revista de la Asociación Geológica Argentina*
529 33, 211–232.
- 530 Favier-Dubois, C.M. and Kokot, R. 2011: Changing scenarios in Bajo de la Quinta (San
531 Matías Gulf, Northern Patagonia, Argentina): impact of geomorphologic processes
532 in subsistence and human use of coastal habitats. *Quaternary International* 245,
533 103–110.
- 534 Feruglio, E. 1933: I terrazzi marini della Patagonia. *Giornali di Geologia Bologna*, 8
535 *bis*, 3–288.
- 536 Feruglio, E. 1950: *Descripción Geológica de la Patagonia. Tomo III*. 432p.
- 537 Fucks, E.E., Schnack, E. and Charó, M. 2012: Aspectos geológicos y geomorfológicos
538 del sector N D del Golfo San Matías, Río Negro, Argentina. *Revista de la Sociedad*
539 *Geológica de España* 25, 95–105.
- 540 Gagliardini, D.A., Aliotta, S., Dogliotti, A.I. and Clemente-Colón, P. 2005:
541 Identification of bed forms through ERS SAR images in San Matías Gulf,
542 Argentina. *Journal of Coastal Research* 21, 193–201.
- 543 Gastaldi, M., De Paula, T.S., Narvarte, M.A., Lôbo-Hajdu, G. and Hajdu, E. 2018:
544 Marine sponges (Porifera) from the Bahía San Antonio (North Patagonian Gulfs,
545 Argentina), with additions to the phylogeography of the widely distributed *Cliona*
546 *aff. celata* and *Hymeniacidon perlevis*, and the description of two new species.
547 *Marine Biology Research* 14, 682–716.
- 548 Gimenez, L., Doldan, M.S., Zaidman, P. and Morsan, E.M. 2020a: The potential of
549 *Glycymeris longior* (Mollusca, Bivalvia) as a multi-decadal sclerochronological

- 550 archive for the Argentine Sea (Southern Hemisphere). *Marine Environmental*
551 *Research* 155, 1–9.
- 552 Gimenez, L., Doldan, M.S., Zaidman, P. and Morsan, E.M. 2020b: Age and growth of
553 *Glycymeris longior* (Sowerby, 1832) clam at the southern edge of its distribution.
554 *Helgoland Marine Research* 74, 1–10.
- 555 González Díaz, E.F. and Malagnino, E.C. 1984: Geomorfología. In Ramos, V. A. (ed.),
556 *Geología y Recursos Naturales de La Provincia de Río Negro. Relatorio Del IX*
557 *Congreso Geológico Argentino.*, 347–364. Asociación Geológica Argentina.
- 558 Gordillo, S., Muñoz, D.F., Bayer, M.S. and Malvé, M.E. 2018: How physical and biotic
559 factors affect brachiopods from the Patagonian Continental Shelf. *Journal of*
560 *Marine Systems* 187, 223–234.
- 561 Gordillo, S. 2009: Quaternary marine mollusks in Tierra del Fuego: insights from
562 integrated taphonomic and paleoecologic analysis of shell assemblages in raised
563 deposits. *Anales del Instituto Patagonia* 37, 5–16.
- 564 Gordillo, S., Coronato, A. and Rabassa, J.O. 1993: Late Quaternary evolution of a
565 subantarctic paleofjord, Tierra del Fuego. *Quaternary Science Reviews* 12, 889–897.
- 566 Gowan, E.J., Rovere, A., Ryan, D.D., Richiano, S., Montes, A., Pappalardo, M. and
567 Aguirre, M.L. 2021: Last interglacial (MIS 5e) sea-level proxies in southeastern
568 South America. *Earth System Science Data* 13, 171–197.
- 569 Gregori, D.A., Kostadinoff, J., Strazzere, L. and Raniolo, A. 2008: Tectonic
570 significance and consequences of the Gondwanide orogeny in northern Patagonia,
571 Argentina. *Gondwana Research* 14, 429–450.
- 572 Hammer, Ø., Harper, D.A.T. and Ryan, P. D. 2001. PAST: Paleontological Statistics
573 Software Package for Education and Data Analysis. *Palaeontologia Electronica* 4,
574 9pp.
- 575 Hanor, J.S. 1978: Precipitation of beachrock cements: mixing of marine and meteoric
576 waters vs CO₂ degassing. *Journal of Sedimentary Petrology* 48, 489–501.
- 577 Hine, A.C. 1979: Mechanisms of berm development and resulting beach growth along a
578 barrier spit complex. *Sedimentology* 26, 333–351.
- 579 Hollmann, R. 1966: Tauchbeobachtungen zur Mollusken-Verbreitung und Sediment-
580 Umlagerung im Golf von Neapel. *Neues Jahrbuch für Geologie und Paläontologie*
581 – *Abhandlungen* 125, 499–526.

- 582 Hopley, D. 1986: Beachrock as a sea-level indicator. *In* van de Plassche, O. (ed.), *Sea-*
583 *Level Research: A Manual for the Collection and Evaluation of Data* 6, 157–173.
- 584 Hulton, N.R.J., Purves, R.S., McCulloch, R.D., Sugden, D.E. and Bentley, M.J. 2002:
585 The Last Glacial Maximum and deglaciation in southern South America.
586 *Quaternary Science Reviews* 21, 233–241.
- 587 Isla, F., Schnack, E. and Aliotta, S. 1995: Evolution and sedimentary dynamics of San
588 Antonio Bay, Rio Negro, Argentina. *XI Symposium on Coastal Sedimentology*.
- 589 Isla, M.F., Moyano-Paz, D., FitzGerald, D.M., Simontacchi, L. and Veiga, G.D. 2023:
590 Contrasting beach-ridge systems in different types of coastal settings. *Earth*
591 *Surface Processes and Landforms* 48, 47–71.
- 592 Ituarte, C.F. 1979: Sobre la sexualidad de *Glycymeris longior* (Sowerby)(Mollusca
593 Pelecypoda). *Neotropica* 25, 161–165.
- 594 Kidwell, S. and Bosence, D.W.J. 1991: Taphonomy and time-averaging of marine
595 shelly faunas. *In* Allison, A., Briggs, D. E. G. (eds.), *Taphonomy: Releasing the*
596 *Data Locked in the Fossil Record*, 115–209. Plenum Press, New York.
- 597 Kidwell, S., Fürsich, F.T. and Aigner, T. 1986: Conceptual framework for the analysis
598 and classification of fossil concentrations. *Palaaios* 1, 228–238.
- 599 Kokot, R.R. and Favier-Dubois, C.M. 2017: Evolución geomorfológica de la Bahía de
600 San Antonio, provincia de Río Negro. *Revista de la Asociación Geológica*
601 *Argentina* 74, 315–325.
- 602 Kokot, R. and Favier Dubois, C. 2009: Evolución geomorfológica de la Bahía San
603 Antonio. Río Negro, Argentina. Su importancia para el registro de ocupaciones
604 humanas. *4º Congreso Argentino de Cuaternario y Geomorfología. 2º Reunión*
605 *sobre el Cuaternario de América del Sur*, 125.
- 606 Kokot, R.R., Codignotto, J., Elissondo, M. 2004: Erosión en la costa patagónica por
607 cambio climático. *Revista de la Asociación Geológica Argentina* 59, 715–726.
- 608 Kowalewski, M., Flessa, K.W. and Hallman, D.P. 1995: Ternary taphograms: triangular
609 diagrams applied to taphonomic analysis. *Palaaios* 10, 478–483.
- 610 Lanfredi, N.W. and Pousa, J.L. 1988: *Mediciones de corrientes, San Antonio Oeste,*
611 *Provincia de Río Negro. San Antonio Oeste, .*
- 612 Lescinsky, H.L., Edinger, E. and Risk, M.J. 2002: Mollusc shell encrustation and
613 bioerosion rates in a modern epeiric sea: taphonomy experiments in the Java Sea,
614 Indonesia. *Palaaios* 17, 171–191.

- 615 Lopes, R.P., Simone, L.R.L., Dillenburg, S.R., Schultz, C.L. and Pereira, J.C. 2013: A
616 middle Pleistocene marine molluscan assemblage from the Southern coastal plain
617 of Rio Grande do Sul State. *Revista Brasileira de Paleontologia* 16, 343–360.
- 618 López, R.A., Penchaszadeh, P.E. and Marcomini, S.C. 2008: Storm-Related strandings
619 of mollusks on the northeast coast of Buenos Aires, Argentina. *Journal of Coastal*
620 *Research* 244, 925–935.
- 621 Lorenzo, N. and Verde, M. 2004: Estructuras de bioerosión en moluscos marinos de la
622 formación Villa Soriano (Pleistoceno tardío-Holoceno) de Uruguay. *Revista*
623 *Brasileira de Paleontologia* 7, 319–328.
- 624 Martínez, H., Nañes, C., Lizuain, A., Dal Molin, C. and Turel, A. 2001: Geological map
625 4166-II San Antonio Oeste. Provincia de Río Negro. *SegemAR*.
- 626 Martínez, S., del Río, C.J. and Rojas, A. 2016: A Pleistocene (MIS 5e) mollusk
627 assemblage from Ezeiza (Buenos Aires Province, Argentina). *Journal of South*
628 *American Earth Sciences* 70, 174–187.
- 629 Mauz, B., Vacchi, M., Green, A., Hoffmann, G. and Cooper, A. 2015: Beachrock: a tool
630 for reconstructing relative sea-level in the far-field. *Marine Geology*.
- 631 Molenaar, N. and Venmans, A.A.M. 1993: Calcium carbonate cementation of sand: a
632 method for producing artificially cemented samples for geotechnical testing and a
633 comparison with natural cementation processes. *Engineering Geology* 35, 103–
634 122.
- 635 Moreira, D., Simionato, C.G. and Dragani, W. 2011: Modeling ocean tides and their
636 energetics in the North Patagonia gulfs of Argentina. *Journal of Coastal Research*
637 27, 87–102.
- 638 Moreira, D., Simionato, C.G., Dragani, W.C. and Nuandñez, M.N. 2009: Tidal and
639 Residual Currents Observations at the San Matías and San José Gulfs, Northern
640 Patagonia, Argentina. *Journal of Coastal Research* 254, 957–968.
- 641 Moresby, C. 1835: Extracts from Commander Moresby's Report on the Northern Atolls
642 of the Maldivas. *The Journal of the Royal Geographical Society of London* 5, 398–
643 404.
- 644 Mouzo, F.H. 2014: Edad del golfo San Matías, Plataforma Continental Argentina y la
645 estratigrafía en el Gran Bajo de San Antonio, provincia de Río Negro. *Revista de la*
646 *Asociacion Geologica Argentina* 71, 125–138.

- 647 Parsons-Hubbard, K.M., Callender, W.R., Powell, E.N., Brett, C.E., Walker, S.E.,
648 Raymond, A.L. and Staff, G.M. 1999: Rates of burial and disturbance of
649 experimentally- deployed molluscs: implications for preservation potential.
650 *Palaios* 14, 337–351.
- 651 Parsons, K. and Brett, C. 1991: Taphonomic processes and biases in modern marine
652 environments: an actualistic perspective on fossil assemblage preservation. *In*
653 Donovan, S. (ed.), *The Processes of Fossilization*, 22–65. Columbia University
654 Press, New York.
- 655 Pascual, M.S., Zampatti, E. and Iribarne, O. 2001: Population structure and demography
656 of the puelche oyster (*Ostrea puelchana*, D’Orbigny, 1841) grounds in Northern
657 Patagonia, Argentina. *Journal of Shellfish Research* 20, 1003–1010.
- 658 Peyrot-Clausade, E.M., Lecampion-Alsumard, T., Hutchings, P., Lecampion, J., Payri,
659 C. and Fontaine, M. 1995: Initial bioerosion and bioaccretion on experimental
660 substrates in high island and atoll lagoons (French Polynesia). *Oceanologica Acta*
661 18, 531–541.
- 662 Pierce, J.W., Sieguel, F.R. and Urien, C.M. 1969: Topografía submarina del Golfo San
663 Matías. *Proceedings of the VI Jornadas Geológicas Argentinas (Buenos Aires,*
664 *Argentina)*, 127–140.
- 665 Ponce, J.F., Rabassa, J., Coronato, A. and Borromei, A.M. 2011: Palaeogeographical
666 evolution of the Atlantic coast of Pampa and Patagonia from the last glacial
667 maximum to the Middle Holocene. *Biological Journal of the Linnean Society* 103,
668 363–379.
- 669 Porro, N. and Fidalgo, F. 1982: *Descripción Geológica de la Hoja 39 J, San Antonio*
670 *Oeste. Provincia de Río Negro*. 96p.
- 671 R Development Core Team. 2023: A Language and Environment for Statistical
672 Computing: R Foundation for Statistical Computing.
- 673 Rhoads, D.C. and Lutz, R.A. 1980: *Skeletal growth of aquatic organisms; Biological*
674 *records of environmental changes*. Plenum Press, New York and London, 750p.
- 675 Ritter, M. do N., Erthal, F. and Coimbra, J.C. 2013: Taphonomic signatures in
676 molluscan fossil assemblages from the Holocene lagoon system in the northern
677 part of the coastal plain, Rio Grande do Sul State, Brazil. *Quaternary International*
678 305, 5–14.
- 679 Ritter, M. do N., Francischini, H., Kuhn, L.A., Da Luz, N.C., Michels, F.H., De Morais,
680 A.L.M., Paim, P.A.V., Xavier, P.L.A. and De Francesco, C.G. 2016. El sesgo del

- 681 operador en la replicabilidad de los estudios tafonómicos comparativos. *Revista*
682 *Brasileira de Paleontologia*, 19, 449–464.
- 683 Rocha, V.P. and Matthews-Cascon, H. 2014: The family Glycymerididae (Mollusca:
684 Bivalvia) from north and northeast Brazil. *Arquivos de Ciências do Mar* 47, 64–71.
- 685 Rodland, D.L., Schöne, B.R., Helama, S., Nielsen, J.K. and Baier, S. 2006: A
686 clockwork mollusc: Ultradian rhythms in bivalve activity revealed by digital
687 photography. *334*, 316–323.
- 688 Ruiz Etcheverry, L.A., Saraceno, M., Piola, A.R. and Strub, P.T. 2016: Sea level
689 anomaly on the Patagonian continental shelf: trends, annual patterns and
690 geostrophic flows. *Journal of Geophysical Research: Oceans* 121, 2733–2754.
- 691 Rutter, N., Radtke, U. and Schnack, E.J. 1990: Comparison of ESR and amino acid data
692 in correlating and dating Quaternary shorelines along the Patagonian coast,
693 Argentina. *Journal of Coastal Research* 6, 391–411.
- 694 Rutter, N., Schnack, E.J., Rio, J. del, Fasano, J.L., Isla, F. and Radtke, U. 1989:
695 Correlation and dating of Quaternary littoral zones along the Patagonian coast,
696 Argentina. *Quaternary Science Reviews* 8, 213–234.
- 697 Santos, A. and Mayoral, E. 2008: Bioerosion versus colonisation on Bivalvia: A case
698 study from the Upper Miocene of Cacela (southeast Portugal). *Geobios* 41, 43–59.
- 699 Scarabino, F., Zaffaroni, J.C., Clavijo, C., Carranza, A. and Nin, M. 2006: Bivalvos
700 marinos y estuarinos de la costa uruguaya: Faunística, distribución, taxonomía y
701 conservación. In Menafra, R., Rodríguez-Gallego, L., Scarabino, F., Conde, D.
702 (eds.), *Bases Para La Conservación y El Manejo de La Costa Uruguaya.*, 157–
703 169. Vida Silvestre. Uruguay (Sociedad Uruguaya para la Conservación de la
704 Naturaleza), Montevideo.
- 705 Scarabino, V. 1977: Moluscos del Golfo San Matías (Provincia de Río Negro,
706 República Argentina). Inventario y claves para su identificación. *Comunicaciones*
707 *de la Sociedad Malacológica de Uruguay* 4, 177–285.
- 708 Schmalz, R.F. 1971: Formation of beach rock at Eniwetok Atoll. In Bricker, O. P. (ed.),
709 *Carbonate Cements*, 17–24. Johns Hopkins University Press, Maryland.
- 710 SHN, Servicio de Hidrografía Naval. 2018. Downloaded from
711 http://www.hidro.gov.ar/oceanografia/Tmareas/RE_Mareas.asp .

- 712 Smith, A.M. and Nelson, C.S. 2003: Effects of early sea-floor processes on the
713 taphonomy of temperate shelf skeletal carbonate deposits. *Earth-Science Reviews*
714 63, 1–31.
- 715 de Souza, R.C.C.L., Lima, T.A. and Silva, E.P. 2010: Holocene molluscs from Rio de
716 Janeiro state coast, Brazil. *Check List* 6, 301–308.
- 717 Stoddart, D.R. and Cann, J.R. 1995: Nature and origin of beach rock. *Journal of*
718 *Sedimentary Petrology* 35, 243–273.
- 719 Tamura, T. 2012. Beach ridges and prograded beach deposits as palaeoenvironment
720 records. *Earth-Science Reviews* 114, 279–297.
- 721 Taylor, M.J. and Stone, G.W. 1996. Beach-ridges: a review. *Journal of Coastal*
722 *Research* 12, 612–621.
- 723 Tonini, M.H. and Palma, E.D. 2011: Respuesta barotrópica de los golfos norpatagónicos
724 argentinos forzados por mareas y vientos. *Latin American Journal of Aquatic*
725 *Research* 39, 481–498.
- 726 Turner, J.C.M. and Baldis, B.A.J. 1978: La estructura transcontinental del límite
727 septentrional de la Patagonia. *VII° Congreso Geológico Argentino, Actas* 2, 225–
728 238.
- 729 Turner, R.J. 2005: Beachrock. In Schwartz, M. L. (ed.), *Encyclopedia of Coastal*
730 *Science*, 183–186. Kluwer Academic Publishers.
- 731 Voudoukas, M.I., Velegrakis, A.F. and Plomaritis, T.A. 2007: Beachrock occurrence,
732 characteristics, formation mechanisms and impacts. *Earth-Science Reviews* 85, 23–
733 46.
- 734 Walker, S.E., Parsons-Hubbard, K., Powell, E.N. and Brett, C.E. 1998: Bioerosion or
735 bioaccumulation? Shelf-slope trends for epi- and endobionts on experimentally
736 deployed gastropod shells. *Historical Biology* 13, 61–72.
- 737 Warton, D.I., Wright, S.T. and Wang, Y. 2012: Distance-based multivariate analyses
738 confound location and dispersion effects. *Methods in Ecology and Evolution* 3, 89–
739 101.
- 740 WoRMS Editorial Board. 2023: *World Register of Marine Species*.
- 741 Zelaya, D.G. 2015: Marine bivalves from the Argentine coast and continental shelf:
742 species diversity and assessment of the historical knowledge. *American*
743 *Malacological Bulletin* 33, 245–62.

744 Zuschin, M., Stachowitsch, M. and Stanton, R.J. 2003: Patterns and processes of shell
745 fragmentation in modern and ancient marine environments. *Earth-Science Reviews*
746 63, 33–82.

747

748 **Appendices**

749 **Figure captions**

750 **Figure 1. 1**, location map of the study area showing the Punta Delgado deposits in the
751 Punta Delgado spit bar, on the western side of San Antonio Bay, SMG (Argentina).

752 **Star** points Punta Delgado samples, **dots** point San Antonio Oeste (SAO) and Las
753 Grutas cities, and **square** points Alpat plant; **2-3** show mapped curvilinear and
754 longitudinal beach ridges (yellow dotted line) at Punta Delgado spit bar (2) and Punta
755 Perdices (3).

756

757 **Figure 2. 1**, contour map showing the location of the San Matias Gulf (SMG) semi-
758 enclosed basin and the Salinas Trapalcó Laguna Curicó Lineament trend; **2**, geological
759 map (from Martinez *et al.* 2001) of San Antonio Bay, SMG (Argentina); **3**,
760 geomorphology of the San Antonio Bay (modified from Angulo *et al.* 1981) with
761 samples location (star). Note that samples are located in Punta Delgado which
762 corresponds to the western spit bar.

763

764 **Figure 3.** Field photographs of the study site. **1**, westwards view of San Antonio Bay at
765 spring tide. Bay is completely flooded, star points sampling site (PD 2016); **2**, eastwards
766 view of San Antonio Bay at spring tide. The dotted line points to the drift line that is
767 located below the beach ridge; **3**, San Antonio Bay at low tide, northwards view from
768 sampling point. The picture was taken standing on the sampling area; the beach ridge is
769 the limit of spring tide; **4**, close up view of a beach ridge showing one shell assemblage
770 dominated by *Glycymeris longior* valves; **5**, close up of the sampling site (PD 2016) in

771 the Punta Delgado deposit, see partial thickness of the deposits; **6**, sampling point detail,
772 densely packed. Scale bars = 20 cm.

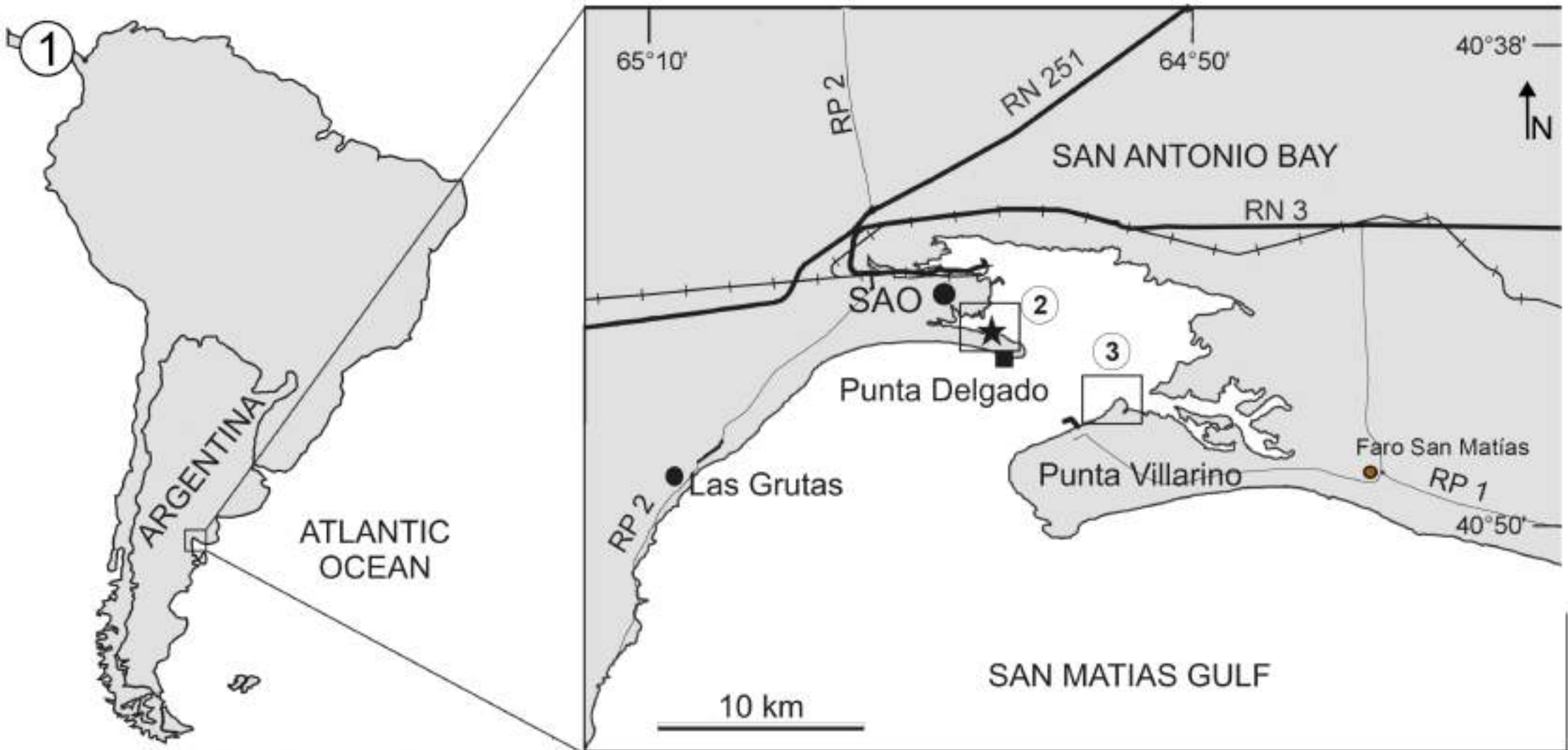
773

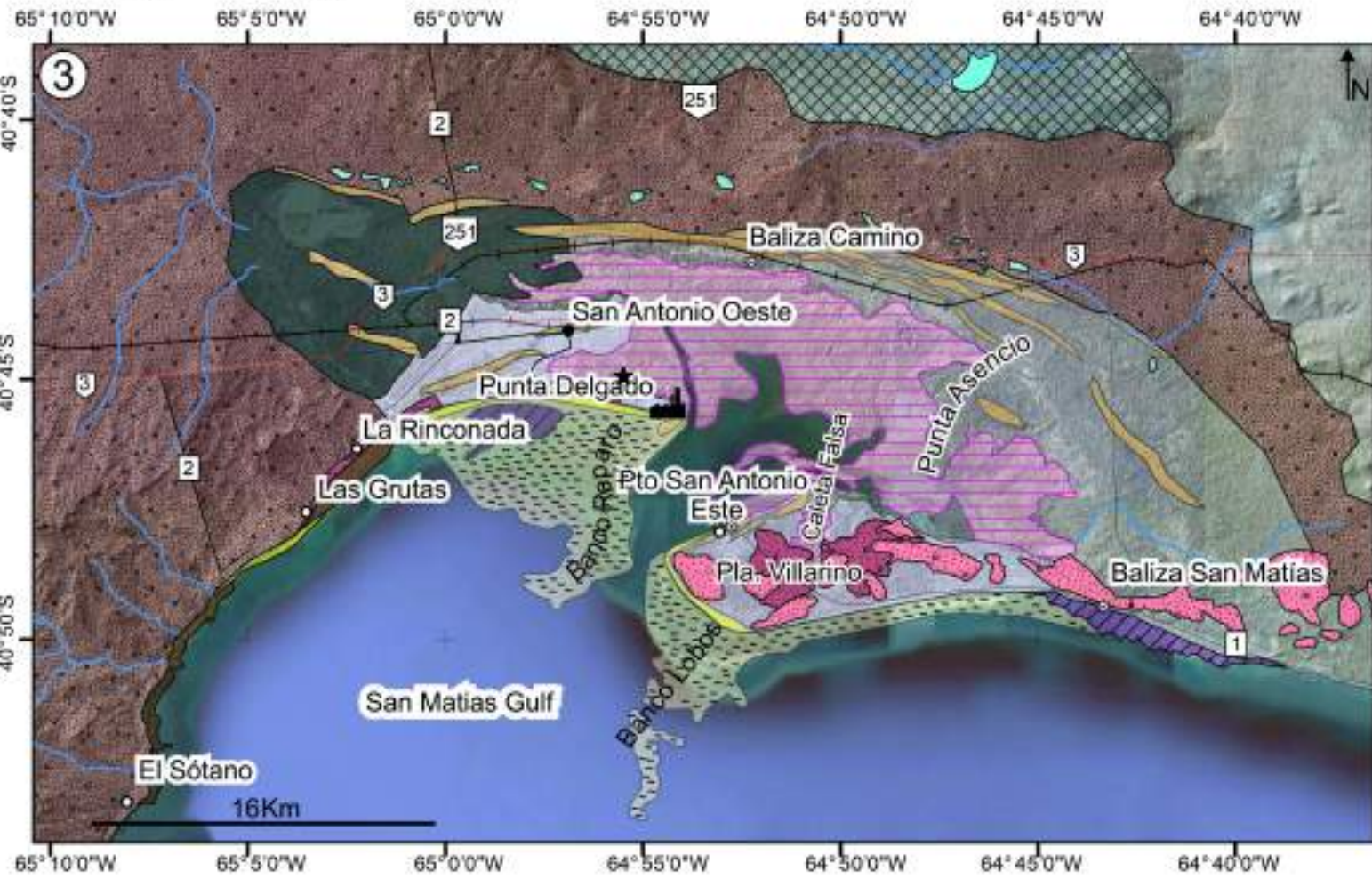
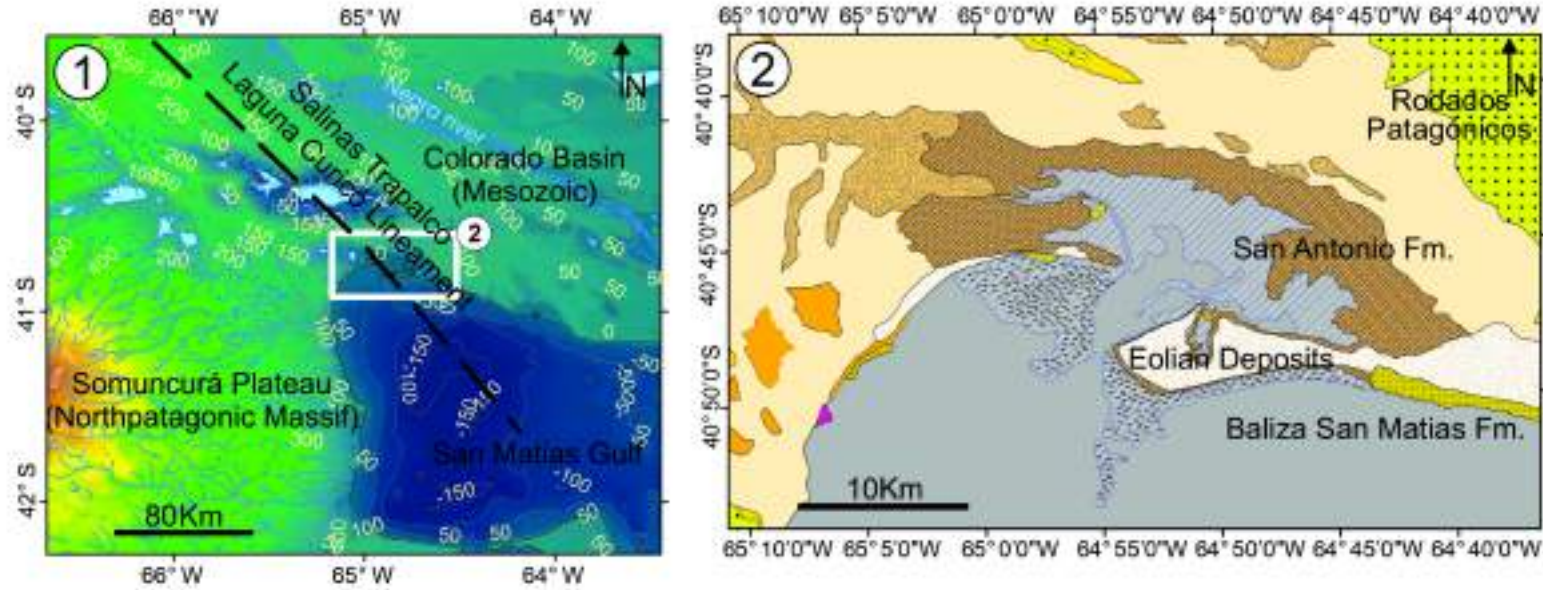
774 **Figure 4.** Taphonomic attributes of *G. longior* valves. Fragmentation: 0, not fragmented
775 shell; 1, shell showing less than 30% of fragmentation; 2, shell showing more than 30%
776 of fragmentation. Rounded; No corroded (and no rounded); Corroded; Internal
777 cementation; External cementation; Post-mortem trace. Scale bars = 1 cm.

778

779 **Figure 5.** Non-metric multidimensional scaling (nMDS) illustrating Punta Delgado
780 shells and groups (samples) formed by taphonomic attributes on a two-dimensional
781 space.

782





Legend

- ★ Study site
- City
- Road
- National Road
- Railway
- River
- Alpat plant.

Geological Units (Fig. 2.2)

- | | |
|-----------------------------------|------------------------|
| Pailemán plutonic complex (C-P) | San Antonio Fm. (Q) |
| Arroyo Barbudo Fm. (K-Pc) | Colluvial deposits (Q) |
| Gran Bajo del Gualicho Fm. (Pt-N) | Alluvial deposits (Q) |
| Río Negro Fm. (N) | Eolian deposits (Q) |
| Rodados Patagónicos (N) | Sandy Tidal Delta |
| Baliza San Matias Fm. (Q) | Tidal Marsh |

Geomorphology (Fig. 2.3)

- | | |
|---------------------|-------------------|
| Semi-enclosed basin | Active Dunes |
| Lagoon | Fossil Dunes |
| Depression | Wave-cut platform |
| Undifferentiated | Spits Bars |
| Abrasion platforms | Beach ridges |
| Beach | Sandy Tidal Delta |
| Pleistocene Beach | Tidal Marsh |

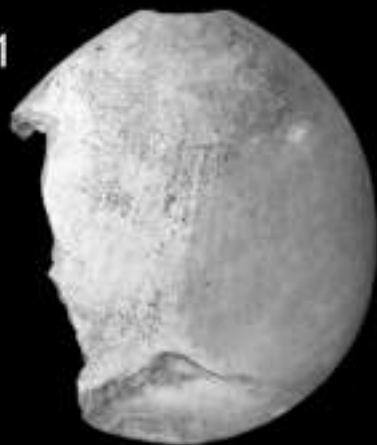


Fragmentation

0



1



2



Rounded



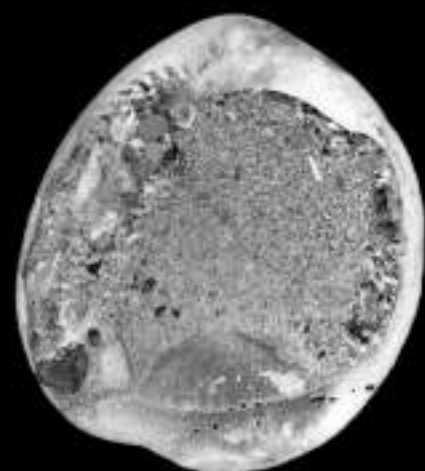
No corroded



Corroded



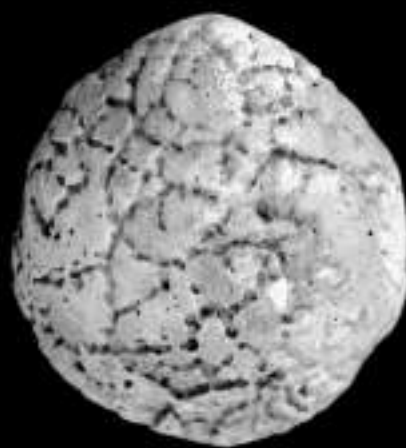
Internal cementation

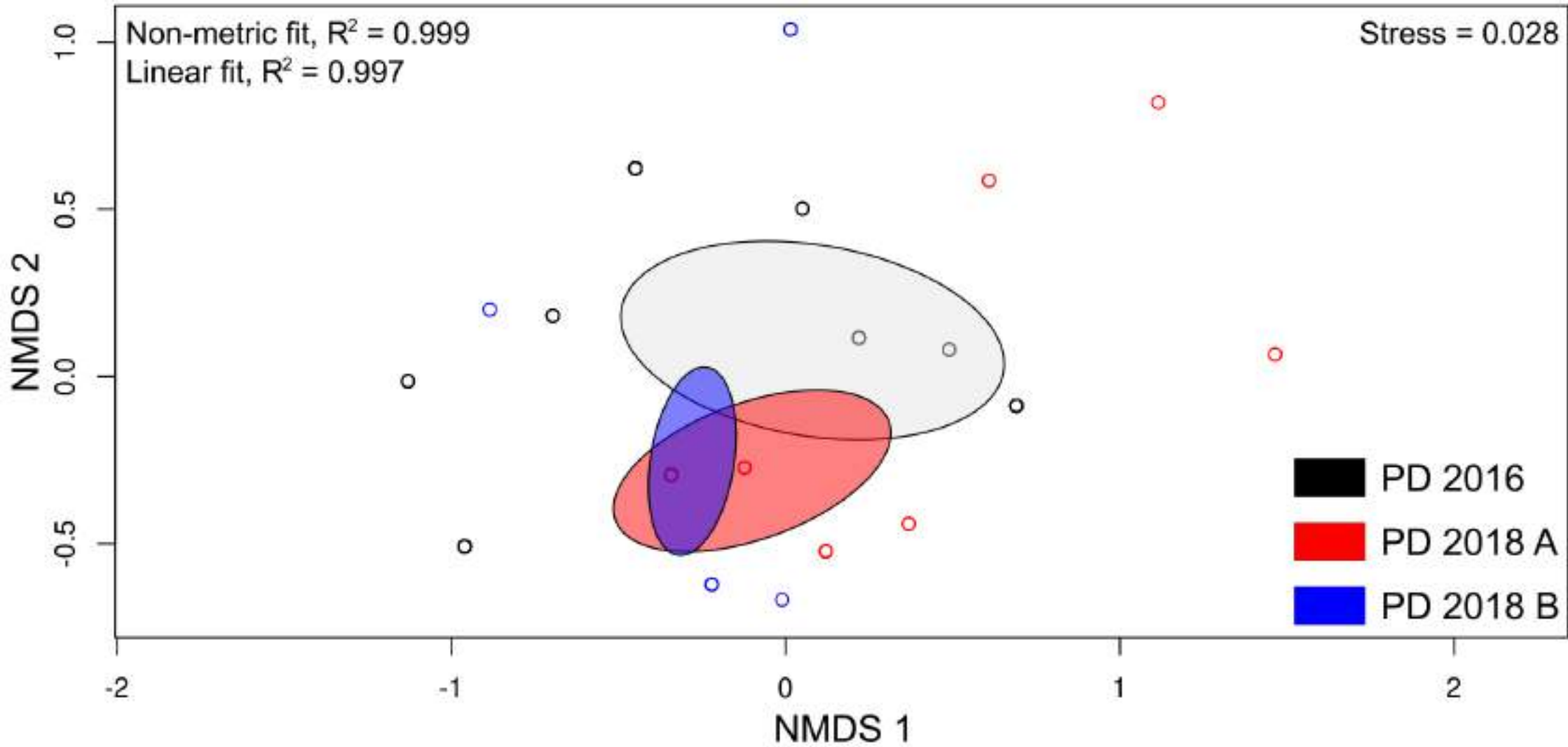


External cementation



Post-mortem trace





PD 2016

PD 2018A

PD 2018B

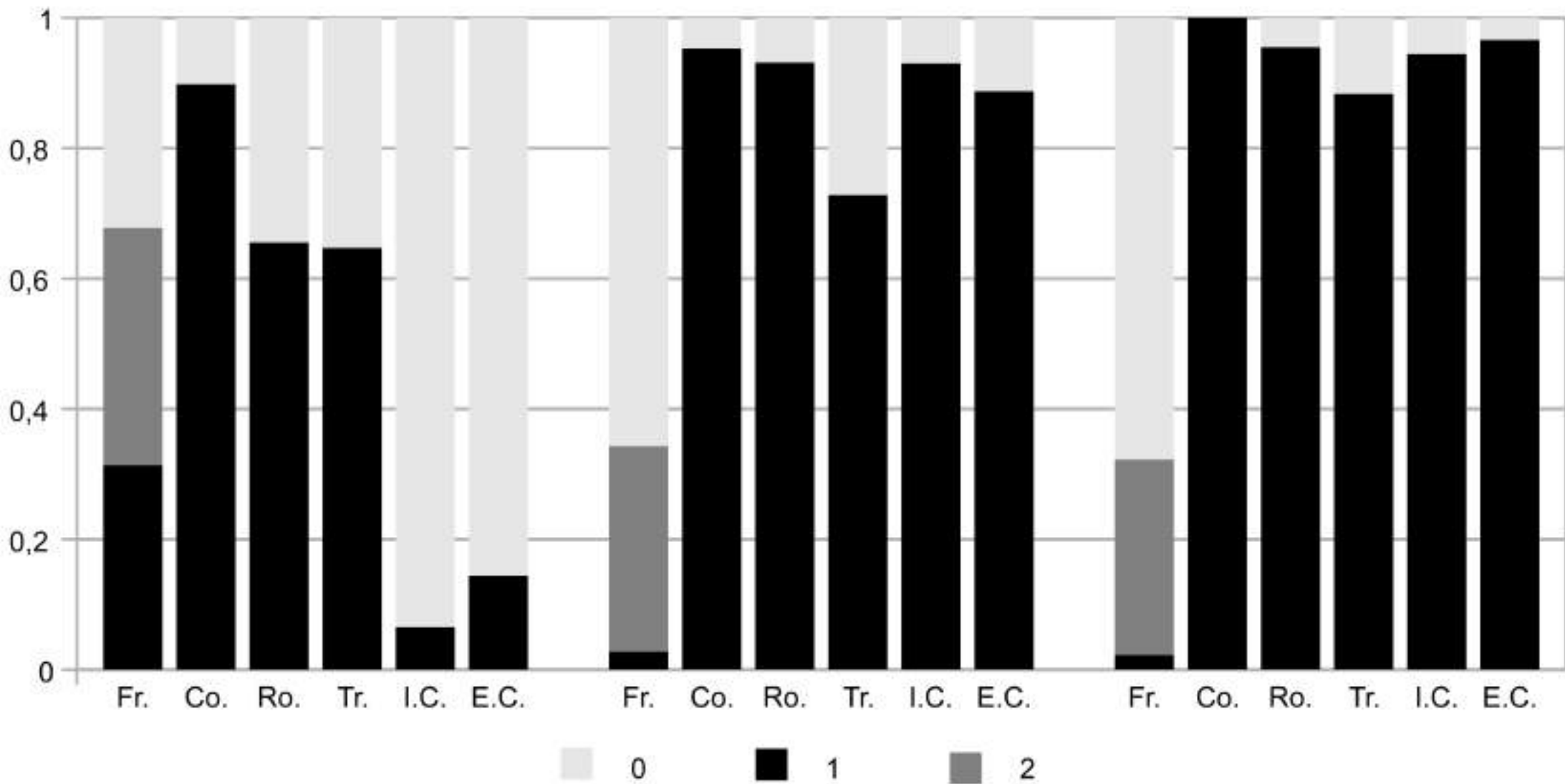


TABLE 1. Percentages of taphonomic attributes per sample.

	Fragmentation		Corrosion		Roundness	<i>Post-mortem</i> traces	Internal Cementation	External Cementation
	0	1	0	1	1	1	1	1
PD 2016	5.93	94.07	10.17	89.83	64.41	64.69	6.50	14.41
PD 2018A	30.14	69.87	4.11	83.56	93.15	69.86	91.78	86.30
PD 2018B	14.61	86.51	0	100	96.63	76.40	94.38	95.51